

First Search for $K_L \rightarrow \pi^0\pi^0\nu\bar{\nu}$.

J. Nix¹, J.K. Ahn², Y. Akune³, V. Baranov⁴, M. Doroshenko^{5,a}, Y. Fujioka³, Y.B. Hsiung⁶, T. Inagaki⁷, S. Ishibashi³, N. Ishihara⁷, H. Ishii⁸, E. Iwai⁹, T. Iwata⁹, S. Kobayashi³, T.K. Komatsubara⁷, A.S. Kurilin⁴, E. Kuzmin⁴, A. Lednev^{1,b}, H.S. Lee², S.Y. Lee², G.Y. Lim⁷, T. Matsumura¹⁰, A. Moisseenko⁴, H. Morii¹², T. Morimoto⁷, T. Nakano¹¹, T. Nomura¹², M. Nomachi⁸, H. Okuno⁷, K. Omata⁷, G.N. Perdue¹, S. Perov⁴, S. Podolsky^{4,c}, S. Porokhovoy⁴, K. Sakashita^{8,a}, N. Sasao¹², H. Sato⁹, T. Sato⁷, M. Sekimoto⁷, T. Shinkawa¹⁰, Y. Sugaya⁸, A. Sugiyama³, T. Sumida¹², Y. Tajima⁹, Z. Tsamalaidze⁴, T. Tsukamoto^{3,*}, Y. Wah¹, H. Watanabe^{1,a}, M. Yamaga^{7,d}, T. Yamanaka⁸, H.Y. Yoshida⁹, and Y. Yoshimura⁷

¹Enrico Fermi Institute, University of Chicago, Chicago, Illinois 60637, USA

²Department of Physics, Pusan National University, Busan, 609-735 Republic of Korea

³Department of Physics, Saga University, Saga, 840-8502 Japan

⁴Laboratory of Nuclear Problems, Joint Institute for Nuclear Research, Dubna, Moscow Region, 141980 Russia

⁵Department of Particle and Nuclear Research, The Graduate University for Advanced Science (SOKENDAI), Tsukuba, Ibaraki, 305-0801 Japan

⁶Department of Physics, National Taiwan University, Taipei, Taiwan 10617 Republic of China

⁷Institute of Particle and Nuclear Studies, High Energy Accelerator Research Organization (KEK), Tsukuba, Ibaraki, 305-0801 Japan

⁸Department of Physics, Osaka University, Toyonaka, Osaka, 560-0043 Japan

⁹Department of Physics, Yamagata University, Yamagata, 990-8560 Japan

¹⁰Department of Applied Physics, National Defense Academy, Yokosuka, Kanagawa, 239-8686 Japan

¹¹Research Center of Nuclear Physics, Osaka University, Ibaragi, Osaka, 567-0047 Japan

¹²Department of Physics, Kyoto University, Kyoto, 606-8502 Japan
(E391a collaboration)

(Dated: December 15, 2018)

The first search for the rare kaon decay $K_L \rightarrow \pi^0\pi^0\nu\bar{\nu}$ has been performed by the E391a collaboration at the KEK 12-GeV proton synchrotron. A new upper limit of 4.7×10^{-5} at the 90 % confidence level was set for the branching ratio of the decay $K_L \rightarrow \pi^0\pi^0\nu\bar{\nu}$ using about 10 % of the data collected during the first period of data taking. First limits for the supersymmetric decay mode $K_L \rightarrow \pi^0\pi^0P$ were also set.

The decay $K_L \rightarrow \pi^0\pi^0\nu\bar{\nu}$ is a Flavor Changing Neutral Current process [1] involving a $s \rightarrow d\nu\bar{\nu}$ transition. In the standard model it is a predominately CP conserving mode with the branching ratio proportional to ρ^2 parameter in the Wolfenstein parameterization of the CKM matrix. The predicted branching ratio in the standard model is $(1.4 \pm 0.4) \times 10^{-13}$ [2]. In this Letter, we report the first experimental limit on this mode. Additionally, we set limits on the supersymmetric mode $K_L \rightarrow \pi^0\pi^0P$, where P is the pseudoscalar sgoldstino [4].

The spontaneous breaking of any global symmetry results in a massless Nambu-Goldstone mode with the same quantum numbers as the symmetry generator. In the case of supersymmetry, the symmetry generator is fermionic resulting in a Nambu-Goldstone fermion, the goldstino. The goldstino has a superpartner, the sgoldstino, which has scalar and pseudoscalar components. If the pseudoscalar sgoldstino is light enough ($m_P < m_{K_L} - 2m_{\pi^0}$) and the quark-sgoldstino is parity preserving, then there should be the decay $K_L \rightarrow \pi^0\pi^0P$. These conditions are met in a variety of models. An upper bound on the branching ratio of this decay of $\approx 10^{-3}$ can be derived from limits on the mass difference between K_L and K_S [4].

The E391a experiment at the KEK 12-GeV proton synchrotron is a dedicated experiment for the decay

$K_L \rightarrow \pi^0\nu\bar{\nu}$ [3]. The first run of data taking took place from February to June 2004. The analysis in this Letter corresponds to approximately 10% of this data. The experiment uses a neutral beam extracted at 4° from the primary proton line. The beam was collimated into a circular beam with a 2 mrad half cone angle [5]. The detector apparatus consists of a CsI crystal calorimeter and 4π hermetic photon veto system. The photon vetoes are arranged cylindrically around the beamline. The primary detectors are contained within a vacuum vessel. The fiducial decay region is kept at a pressure of 1×10^{-5} Pa. This central region is separated from the rest of the detector by a vacuum membrane. This membrane was not properly secured during Run I and hung into the beam line at the charged veto ≈ 50 cm upstream of the CsI face. The front barrel (FB) begins 11 m downstream of the target, which we define as the 0 point of our Z -coordinate. A diagram of the detector cross section is shown in Fig. 1.

The calorimeter consists of 576 blocks of undoped CsI crystals. The majority of crystals are $7 \times 7 \times 30$ cm³ blocks. There are 24 $5 \times 5 \times 50$ cm³ crystals surrounding the beam hole [7]. The face of the CsI array is located at a Z position of 614.8 cm. In front of the CsI is a charged veto system consisting of 32 overlapping 6 mm thick plastic scintillator located at 550 cm.

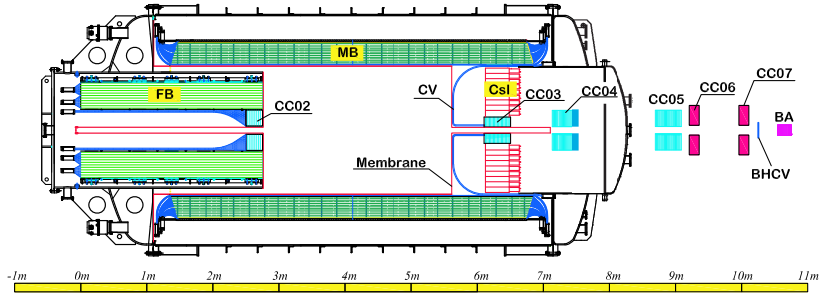


FIG. 1: Cross section of the E391a detector. K_L^0 's enter from the left side.

There are multiple veto detectors making up the 4π photon veto system. The Main Barrel is the primary photon veto surrounding the fiducial decay region. It is made of lead-scintillator sandwich with an inner diameter of 2.0 m and is $13.9 X_0$ thick.

The photon vetoes were calibrated using either cosmic ray or beamline muons. The CsI array was calibrated during a special run using a 5 mm Al target to produce π^0 's with a known position. This calibration is matched to cosmic ray muon data which is used to track changes in gain over time.

The experimental signature of both $K_L \rightarrow \pi^0\pi^0\nu\bar{\nu}$ and $K_L \rightarrow \pi^0\pi^0P$ is four photons in the final state with missing mass and high transverse momentum, P_T . The energy and hit position of the 4γ are measured by our calorimeter. Photons are reconstructed by summing the energy of contiguous blocks with energy deposited and the position of the photon is calculated by using the distribution of energy deposited in the CsI blocks.

The possible π^0 decay vertices can be reconstructed assuming the decay occurred on the beam axis. The best solution is selected from the multiple possible pairings of photons and π^0 's, by choosing the minimum χ^2 of the Z separation of the $2\pi^0$. The signal modes are distinguished by their relatively high P_T and reconstructed invariant masses below that of the K_L .

The kaon flux was calculated by measuring $K_L \rightarrow \pi^0\pi^0$. It was cross-checked by measuring $K_L \rightarrow \pi^0\pi^0\pi^0$. The acceptance of these modes was calculated using a GEANT based Monte Carlo [8]. The simulation included an overlay of accidental events selected from data. The acceptances and fluxes for these modes are shown in Table I.

The acceptance of the mode $K_L \rightarrow \pi^0\pi^0P$ depends on the mass of the P . As the mass increases there is a decline in acceptance due to the reduction in the maximum P_T of the $2\pi^0$'s. This eventually leads to the phase space of the decay to lie completely in the region of high $K_L \rightarrow \pi^0\pi^0\pi^0$ background. The single event sensitivity as a function of sgoldstino mass is shown in Fig. 2.

The signal box was defined by the P_T of the reconstructed kaon, the invariant mass of the $\pi^0 - \pi^0$ system, and the reconstructed decay vertex. The acceptable P_T was defined to be between 100 and 200 MeV/ c^2 . The lower bound was dictated by the presence of large

amounts of $3\pi^0$ background at lower values of P_T . The invariant mass of the reconstructed kaon was required to be between 268 and 450 MeV/c. The lower bound is set by the minimal reconstructed mass with the intermediate reconstruction of two pions and the upper bound is set by the presence of $K_L \rightarrow \pi^0\pi^0$ mass peak at the kaon's true mass of 498 MeV/c. The acceptable decay vertices are between 300 and 500 cm. The upstream limit of 300 cm is set by the presence of halo neutrons interacting with CC02 at 275 cm. The downstream limit of 500 cm is set by core neutrons interacting with the vacuum membrane at ≈ 550 cm.

Mode	Acceptance	Flux
$\pi^0\pi^0$	$(2.16 \pm 0.13) \times 10^{-4}$	$(1.54 \pm 0.04) \times 10^9$
$\pi^0\pi^0\pi^0$	$(1.39 \pm 0.07) \times 10^{-6}$	$(1.57 \pm 0.04) \times 10^9$
$\pi^0\pi^0\nu\bar{\nu}$	$(5.33 \pm 0.23) \times 10^{-5}$	NA

TABLE I: Acceptance and flux calculations of different signal modes. Acceptance is the signal acceptance calculated from Monte Carlo. Flux is the number of kaon decays in the fiducial region.

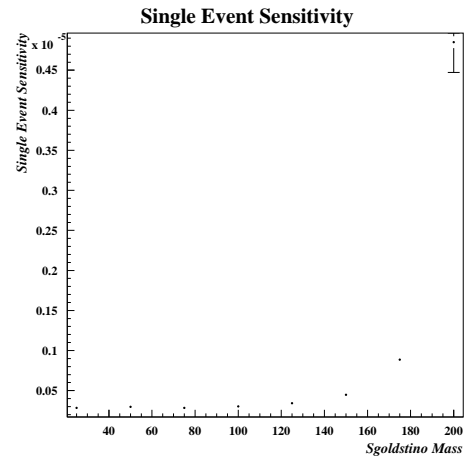


FIG. 2: Single event sensitivity for $K_L \rightarrow \pi^0\pi^0P$ decay for differing sgoldstino masses.

There are two important sources of background to the signal: $K_L \rightarrow \pi^0\pi^0\pi^0$ with missing photons, and neutron related backgrounds. We predicted the backgrounds from data using a bifurcation technique [9],[10]. The number of observed background events can be factored into the number of events after applying a group of setup cuts, N_0 , and the probability of one of these events surviving the remaining cuts. If we break up the remaining cuts into two uncorrelated groupings, A and B, this probability can be factored into the probabilities of surviving each set, $P(A)$ and $P(B)$. We can rewrite this in terms of the number of events surviving the application of each cut and the inverse of the other and the events which survive the application of the inverse of both cuts,

$$N_{\text{bkg}} = N_{A\bar{B}}N_{\bar{A}B}/N_{\bar{A}\bar{B}}. \quad (1)$$

The primary source of background is $K_L \rightarrow \pi^0\pi^0\pi^0$. There are three channels for this decay to produce background: two photons lost due to either geometric or detector inefficiency, one photon missing and one photon fusions in the CsI, or two photon fusions in the CsI. However, these three types of events all have similar cut survival probabilities and therefore can be treated as one source of background in our bifurcation analysis. Our cut set A consists of photon veto cuts. Cut set B is made up of cuts on the quality of the photon cluster and the reconstruction.

To check the bifurcation methodology, we applied it to regions surrounding the signal box. The Low P_T region is defined by same bounds in Z and invariant mass as the signal region and a P_T between 50 and 100 MeV/c. The High Mass region is defined by the same bounds in Z and P_T as the signal region and a mass between 450 and 550 MeV/c². The High and Low Z regions have the same bounds in invariant mass and P_T as the signal region and have reconstructed vertices between 500 to 550 cm and 250 to 300 cm, respectively. The predictions for these regions agree fairly well with data as shown in Table II.

For this technique to correctly predict the background, the cut sets A and B need to be uncorrelated. We selected cuts on this basis, but there is some correlation. An estimate of the error caused by ignoring this correlation can be made with values which do not require opening the signal box as

$$C_\epsilon = \epsilon \times N_{\bar{A}\bar{B}} \left(1 + \frac{N_{\text{pred.}}}{N_{\bar{A}\bar{B}}}\right). \quad (2)$$

Here ϵ is the difference in cut survival probability between cut A for an event passing cut B and an event passing the inverse of B. We determined ϵ using events in the Low P_T region. We estimate this as a systematic error of 0.12 background events.

Another important source of systematic error in the bifurcation analysis is contamination of other background sources in the signal region, primarily neutron related backgrounds. If there is a second background source with different veto survival probabilities there is a correction

to the prediction. It takes the form of

$$N_{\text{bkg}} = \frac{N_{A\bar{B}}N_{\bar{A}B}}{N_{\bar{A}\bar{B}}} + \frac{N_1N_2}{N_{\bar{A}\bar{B}}} \Delta_A \Delta_B, \quad (3)$$

Here, N_1 and N_2 are the number of events of each background type before cuts A and B are applied, and Δ_A and Δ_B are the difference in the veto probabilities between the background types for the two cuts. It is important to note that the correction term does not directly correspond to the background contribution from the secondary sources. The largest source of neutrons is the interaction of beam core neutrons with the vacuum membrane in front of the Charged Veto. A second source is the interaction of halo neutrons with CC02 before the fiducial decay region. Both of the sources produce reconstructed events which are localized to their point of origin with high P_T . Both of these regions are outside the fiducial decay region of 300cm < Z < 500cm. To estimate the impact of these events on the the background prediction, it was necessary to determine the number of core neutron background events in the signal box under the setup cuts.

The number of neutron events in the region with Z greater than 500 cm and P_T greater than 0.1 GeV/c is too small to fit when all cuts are applied. We therefore fit using a loose set of cuts. We remove the BA cut, cuts on the distribution of gamma energy and timing, and a veto on additional energy in the CsI. Additionally we apply cuts not-A and not-B to ensure we are not observing events in the signal box while being able to look at events in the Z fiducial region. With these sets of cuts the core neutron peak in the high P_T -high Z region is clearly visible and can be fit with a Gaussian as shown in Figure 3. In the high P_T -fiducial Z region, there is a predominately $K_L \rightarrow \pi^0\pi^0\pi^0$ background. The Gaussian component of the core neutron peak produces a negligible contribution to the background in the fiducial region. The density of this distribution is calculated by subtracting off the $K_L \rightarrow \pi^0\pi^0\pi^0$ contribution found by Monte Carlo and fitting the remainder by a Gaussian plus a straight line. Integrating this function over the fiducial region gives $248 \pm 4_{\text{stat.}} \pm 124_{\text{syst.}}$ core neutron background events with the loose cuts applied. The application of the rest of the setup cuts reduces this by a factor of ≈ 115 . A predicted total core neutron background in the signal region is $2.16 \pm 0.03_{\text{stat.}} \pm 1.05_{\text{syst.}}$ under the setup cuts, before the application of cuts A and B. This corresponds to N_2 in Equation 3.

The cut survival probabilities do differ significantly with $\Delta_A = (26.4 \pm 1.3)\%$ and $\Delta_B = (8.6 \pm 0.5)\%$ which is derived from Monte Carlo studies. This results in an estimation of the error to the background prediction of 0.06 events.

The bifurcation background predictions gives us a total background prediction of $0.43 \pm 0.32_{\text{stat.}} \pm 0.13_{\text{sys.}}$. Opening the signal box, we observe a single event. This is consistent with the background prediction.

The error in the branching ratio of $K_L \rightarrow \pi^0\pi^0$ contributes a systematic error on the order 0.5% to our single

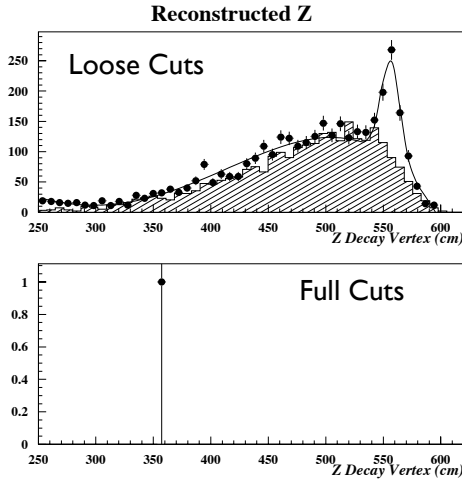


FIG. 3: Z distribution of reconstructed events with $P_T > 100$ MeV/c. Points are data, shaded region represents a scaled $K_L \rightarrow \pi^0 \pi^0 \pi^0$ Monte Carlo sample, and the line is the fitted curve. The top plot shows the distribution with the loose set of cuts from which we derived our neutron background prediction, the bottom plot shows the same distribution with all cuts applied.

TABLE II: Prediction of background events in different regions.

Region	N_{AB}	N_{AB}	N_{AB}	Prediction	Data
Low P_T	380	72	115	21.1 ± 3.3	13
High Mass	46	9	4	0.78 ± 0.48	1
Low Z	5	0	0	0	0
High Z	0	0	6	0	0
Signal	84	18	2	0.43 ± 0.32	1

event sensitivity. Photon veto energy calibration contributes a systematic error 3.7%. Discrepancies between Monte Carlo and data acceptance loss in the cuts, that were simulated by Monte Carlo, give a systematic error of 3.4% in acceptance. The total systematic acceptance

error is 5.0%. Combining the branching ratio and acceptance errors produces a 7.1% systematic error in the single event sensitivity.

Our single event sensitivity for $K_L \rightarrow \pi^0 \pi^0 \nu \bar{\nu}$ is $(1.20 \pm 0.06_{\text{stat.}} \pm 0.09_{\text{sys.}}) \times 10^{-5}$. With 1 observed event, which is consistent with the background prediction, we set a limit at the 90% confidence level for the branching ratio at 4.7×10^{-5} . This is the first limit set on this decay mode. The single event sensitivities for $K_L \rightarrow \pi^0 \pi^0 P$ with different masses are shown in Figure 2. For P masses of less than 100 MeV/c² we can set a limit on $K_L \rightarrow \pi^0 \pi^0 P$ of 1.2×10^{-6} .

*Deceased

^aPresent address: KEK, Tsukuba, Ibaraki, 305-0801

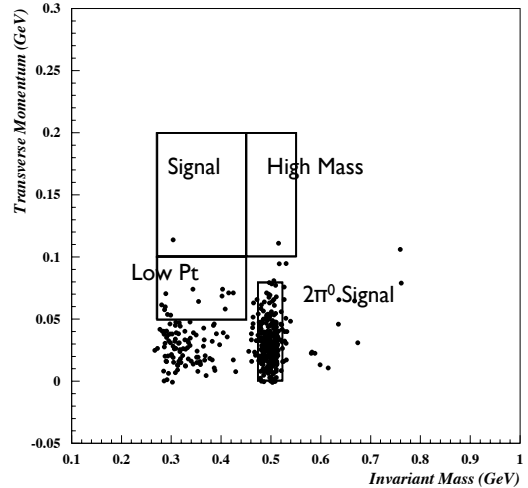


FIG. 4: P_T plotted against mass. The rectangular regions correspond to the regions in Table II.

Japan.

^bAlso Institute for High Energy Physics, Protvino, Moscow region, 142281 Russia.

^cAlso Scarina Gomel' State University, Gomel', BY-246699, Belarus.

^dPresent address: Osaka University, Toyonaka, Osaka, 560-0043 Japan.

[1] L. S. Littenberg and G. Valencia, *Phys. Lett. B* **385**, 379 (1996).
[2] C.W. Chiang and F. J. Gilman, *Phys. Rev. D* **62**, 094026 (2000).
[3] S. Adler *et al.*, *Phys. Rev. L* **79**, 2204 (1997).
[4] D. S. Gorbunov and V. A. Rubakov, *Phys. Rev. D* **64**, 054008 (2001).
[5] H. Watanabe *et al.*, *Nucl. Instr. Meth. A* **545**, 542 (2005).
[6] M. Doroshenko, Ph.D. thesis, The Graduate University

for Advanced Science, 2005; K. Sakashita, Ph.D. thesis, Osaka University, 2006.

[7] M. Doroshenko *et al.*, *Nucl. Instr. Meth. A* **545**, 278 (2005).

[8] R. Brun *et al.*, GEANT 3.21, CERN, Geneva, 1994.

[9] H.K. Park *et al.*, *Phys. Rev. Lett.* **94**:021801 (2005)

[10] J. Nix *et al.*, Enric Fermi Institute Preprint 07-04 (2007)